CELLULAR NEUROSCIENCE

Human endogenous retroviral protein triggers deficit in glutamate synapse maturation and behaviors associated with psychosis

E. M. Johansson[1,2]*, D. Bouchet[1,2†], R. Tamouza[3,4,5†], P. Ellul[1,2,3,4,5], AS. Morr[1,2], E. Avignone[1,2], R. Germi[6], M. Leboyer[3,4,5], H. Perron[7,8], L. Groc[1,2]*

Mobile genetic elements, such as human endogenous retroviruses (HERVs), produce proteins that regulate brain cell functions and synaptic transmission and have been implicated in the etiology of neurological and neurodevelopmental psychiatric disorders. However, the mechanisms by which these proteins of retroviral origin alter brain cell communication remain poorly understood. Here, we combined single-molecule tracking, calcium imaging, and behavioral approaches to demonstrate that the envelope protein (Env) of HERV type W, which is normally silenced but expressed in patients with neuropsychiatric conditions, alters the *N*-methyl-D-aspartate receptor (NMDAR)–mediated synaptic organization and plasticity through glia- and cytokine-dependent changes. Env expression in the developing hippocampus was sufficient to induce behavioral impairments at the adult stage that were prevented by Env neutralization or tuning of NMDAR trafficking. Thus, we show that a HERV gene product alters glutamate synapse maturation and generates behavioral deficits, further supporting the possible etiological interplay between genetic, immune, and synaptic factors in psychosis.

INTRODUCTION

Understanding the molecular and cellular mechanisms underpinning brain cell communication in healthy and diseased brain is one of the major challenges in modern neuroscience. Beside classical neuro- and glio-transmitter systems, proteins of retroviral or transposon origin can modulate brain cell communication (*1*–*3*). For instance, the neuronal gene Arc, with retroviral origin, controls glutamatergic synapse and cognitive functions (*4*–*6*). Mobile genetic elements from the human endogenous retrovirus (HERV) families also have the capacity to control gene regulatory networks during brain evolution and development (*1*, *7*, *8*) and modulate brain cell physiology and communication (*3*). These endogenous retroviruses, which embody around 8% of the human genome, are remnants of infections that took place several million years ago (*2*). Beside these physiological roles, HERV proteins have also been associated with major neurological and psychiatric disorders (*3*, *9*). HERV-K type–derived proteins play a role in the neurodegenerative process observed in patients with amyotrophic lateral sclerosis (ALS) (*10*). A fraction of patients diagnosed with schizophrenia or bipolar disorders express HERV-W genes with variable copy numbers and gene products (*11*–*13*). In brain disorders, it is believed that early immune challenges [e.g., influenza virus, herpes virus, Epstein-Barr virus, and cytomegalovirus, as well as *Toxoplasma gondii* parasite (*3*, *9*, *14*, *15*)] trigger HERV gene expression and subsequent pathological cascades. Yet, the mechanisms by which HERV gene products affect brain cell communication, synaptic transmission, and brain functions remain mostly unknown.

Overactivation of immune cells early in development contributes to the etiology of major neuropsychiatric disorders through major alterations of glutamatergic synapse transmission and maturation and of spine density (*16*, *17*). These deficits in excitatory glutamate synapses are triggered by a corrupted *N*-methyl-D-aspartate receptor (NMDAR)–mediated transmission (*18*, *19*), which constitute the core molecular hypothesis of the etiology of psychotic disorders (*20*, *21*). NMDARs are heterotetramers consisting of the association between the obligatory GluN1 subunit and GluN2A to GluN2D and/or GluN3 subunits, providing specific biophysical and pharmacological properties to each receptor subtype (*19*). In the hippocampus, GluN1 mostly associates with GluN2A and/or GluN2B subunits. During brain development, the synaptic NMDAR composition changes from GluN2B- to GluN2A-rich in an activity-dependent manner, which profoundly affects the plasticity of developing synapses and plays a central role in the fine-tuning of neuronal network formation (*19*). Here, we explore the possibility that proteins of retroviral origins, which are expressed in human brains from patients with neuropsychiatric disorders, perturb glutamatergic synapse transmission and plasticity. We investigated the capacity of the HERV-W envelope (Env) protein, which can be released in the extracellular environment (*11*, *22*, *23*) to alter NMDAR trafficking and organization, neuronal network function, and behavior in rodents. We focus our attention on the hippocampus, whose structure is impaired in major neuropsychiatric disorders (*19*), and it expresses high levels of NMDAR. We provide direct evidence that Env tunes glutamatergic synapse maturation during neurodevelopment and induces psychotic-like behaviors in adult rodents. These findings support the hypothesis that HERV genetic elements represent a putative substrate in psychotic disorders, linking the well-defined immune and synaptic dysfunctions observed in mental illnesses.

[1]Interdisciplinary Institute for Neuroscience, Université de Bordeaux, Bordeaux, France. [2]CNRS, IINS UMR 5297, Bordeaux, France. [3]University Paris Est, Psychiatry Department, Hopitaux Universitaires Henri Mondor, AP-HP, DHU PePSY, Créteil, France. [4]Institut Mondor de Recherche Biomédicale, Translational Psychiatry Laboratory, INSERM U955, Créteil, France. [5]Fondation FondaMental, Créteil, France. [6]IBS, UMR 5075 CEA-CNRS-Université Grenoble-Alpes and CHU Grenoble-Alpes, Grenoble, Créteil, France. [7]GeNeuro, 18, chemin des Aulx, 1228 Plan-les-Ouates, Geneva, Switzerland. [8]Université de Lyon-UCBL, Lyon, France.
*Corresponding author. Email: laurent.groc@u-bordeaux.fr (L.G.); emily.johansson@u-bordeaux.fr (E.M.J.)
†These authors contributed equally to this work.

RESULTS

Recombinant Env disperses synaptic NMDA receptors in hippocampal neurons without interfering with the ionotropic function

To unveil the action of HERV-W Env, which does not exist in the rodent genome, we generated a recombinant Env protein. As most psychotomimetic drugs are NMDAR antagonists (*18*, *20*), we first tested whether Env antagonizes NMDAR-mediated synaptic transmission in hippocampal networks. Neither NMDAR-mediated calcium transients in cultured hippocampal neurons nor evoked NMDAR-mediated excitatory postsynaptic currents in *cornu ammonis* (CA)3-CA1 synapses were altered by various concentrations of Env (Fig. 1, A to C), indicating that Env is not an NMDAR antagonist. As NMDAR hypofunction can be triggered by a physical displacement of the receptors (*19*, *24*), we measured the NMDAR surface diffusion in the presence of Env. Since NMDAR in hippocampal synapses mainly contain GluN2A and GluN2B subunits, we traced each of these endogenous receptor subtypes at the surface of live hippocampal neurons using single nanoparticle [quantum dot (QD)] imaging (Fig. 1D) (*25*). Short exposure (5 min) of Env rapidly and specifically increased GluN2B-NMDAR surface diffusion and mean square displacement (MSD) in the postsynaptic compartment (Homer 1c–positive area) (Fig. 1, D and E, and fig. S1, A to D). This effect is kept after a 24-hour Env exposure (fig. S1, E to H). The presence of a specific Env-neutralizing antibody fully prevented the Env-dependent effect without altering the basal surface diffusion (Fig. 1F and fig. S1, B, D, G, and H). In addition, heat-inactivated Env had no effect (fig. S1, I and J), excluding the nonspecific effect of residual endotoxins. The Env-induced GluN2B-NMDAR dispersal was maintained after blocking neuronal action potentials with tetrodotoxin (TTX) (fig. S1K). Thus, Env rapidly, durably, and laterally disperses synaptic NMDAR in a subunit-specific and neuronal activity–independent manner.

The Env-induced GluN2B-NMDAR dispersal was accompanied by a decrease in the synaptic fraction of GluN2B-NMDAR-nanoparticle complexes (Fig. 1G), likely altering the GluN2A/2B synaptic ratio. Consistently, Env exposure (24 hours) increased the relative amount of synaptic GluN2A-NMDAR (Fig. 1, H to J). Neither the expression of the postsynaptic scaffold protein, PSD-95, nor the dendritic density of glutamatergic synapses were altered after such an exposure to Env (Fig. 1I) (Control, 1.0 ± 0.074, n = 58 neurons; Env, 0.96 ± 0.067, n = 66; means ± SEM; number of PSD-95 clusters/dendrite length, normalized to control: $P > 0.05$), suggesting that Env preserves the overall structure and amount of glutamatergic synapses. These data indicate that Env rapidly alters NMDAR trafficking within synapses, leading to a fast GluN2B-NMDAR dispersal followed by a relative increase in GluN2A-NMDAR.

Env laterally disperses synaptic NMDAR through glia-, TLR-4–, and cytokine-dependent processes

To unveil the mechanism underpinning the Env-mediated NMDAR synaptic disorganization, we based our investigation on the evidence that Env effects in the brain are mainly mediated by Toll-like receptor 4 (TLR-4) and proinflammatory cytokines (*26*). Because TLR-4 is expressed by microglial cells in the brain, we exposed glia-free neuronal cultures (with similar neuronal density but without astrocyte or microglia) with Env. In the absence of glial cells, GluN2B-NMDAR synaptic dynamics remained unchanged upon Env exposure (Fig. 2A and B). Note that the dendritic synapse density was identical in glial-containing and glial-free cultures (glia containing, 0.97 ± 0.051, n = 31 neurons; glia free, 0.97 ± 0.048, n = 31; means ± SEM; nb of exogenous Homer 1c clusters/dendrite length: $P > 0.05$). Env was also ineffective when TLR-4 was blocked in hippocampal networks (including neurons and glia cells) using a specific TLR-4–neutralizing antibody (Fig. 2C and fig. S2, A to C), suggesting that TLR-4 is necessary to trigger the Env effect on NMDAR dynamics. Consistently, the TLR-4 agonist, lipopolysaccharide (LPS), was sufficient to increase synaptic GluN2B-NMDAR surface dynamics (fig. S2D). It could be noted that the magnitude of the microglial activation was distinct between Env and LPS (fig. S2, E to G), suggesting that these two proteins share some, but not all, signaling pathways. In search of the glial mediator(s) of the Env action on neuronal NMDAR, we measured the extracellular levels of cytokines in hippocampal networks after short Env exposure. The levels of the proinflammatory cytokines interleukin-1 (IL-1), IL-6, tumor necrosis factor (TNF-α), and interferon-γ increased (Fig. 2D). To test whether these changes in cytokine levels play an instructive role in the Env-induced synaptic NMDAR dispersal, hippocampal networks were exposed to Env together with various cytokine blockers. Blocking IL-1 with the IL-1 receptor antagonist, IL-ra, fully prevented the Env-induced GluN2B-NMDAR synaptic dispersal (Fig. 2, E and F), whereas blocking IL-6 or TNF-α only had dampening effects (Fig. 2E). Furthermore, IL-1β alone was sufficient to increase GluN2B-NMDAR diffusion in glia-free neuronal cultures (Fig. 2G). We then observed that the dendritic IL-1 receptor (IL-1R) density was increased in response to Env (Fig. 2H). Since activation of IL-1R triggers intracellular protein kinase activation (*27*), such as the Src family tyrosine kinases, we tested whether the presence of the Src family tyrosine kinase blocker PP2 (1 μM) prevented the Env-mediated NMDAR dispersal. Whereas PP2 had no effect on basal GluN2B-NMDAR surface diffusion (pre, 1.0 ± 0.027; post PP2 (15 min), 0.985 ± 0.027, n = 6 neurons; means ± SEM: $P > 0.05$), it prevented the Env-induced increase of GluN2B-NMDAR surface diffusion (Fig. 2I). These data indicate that Env rapidly disperses synaptic GluN2B-NMDAR through a glial-, TLR-4–, and cytokine (predominantly IL-1)–dependent process.

Prolonged Env exposure potentiates glutamatergic synapse transmission and prevents long-term potentiation

GluN2-NMDAR subtypes tune NMDAR transmission at the synaptic and network levels (*19*). Since Env reshuffles GluN2A/B-NMDAR synaptic content, we tested the effect of Env exposure (24 hours) on the NMDAR-mediated basal activity and on NMDAR-dependent long-term synaptic potentiation (LTP). The frequency of NMDAR-mediated Ca^{2+} transients in dendritic spines was increased by approximately 25% (Fig. 3, A and B), consistent with the reported homeostatic upscaling of synaptic activity following glutamatergic hypofunction (*28*). In addition, the synchrony of NMDAR-mediated transients was favored (Fig. 3, C and D), indicating that Env profoundly reshaped the network activity. Consistent with the key role of IL-1β, the network activity change was prevented by IL-1R blockade (Fig. 3, B and D). Because the bulk exposure of extracellular Env may not reflect the bioavailability of the protein within rodent or human brains, we then genetically expressed Env for several days in few hippocampal cells (~3%; Fig. 3E and fig. S3). This scarce expression was sufficient to destabilize synaptic GluN2B-NMDAR (Cont., 0.112 ± 0.028 to 0.224, n = 1173/10 trajectories/neuron; Env, 0.135 ± 0.032 to 0.261, n = 915/10; median

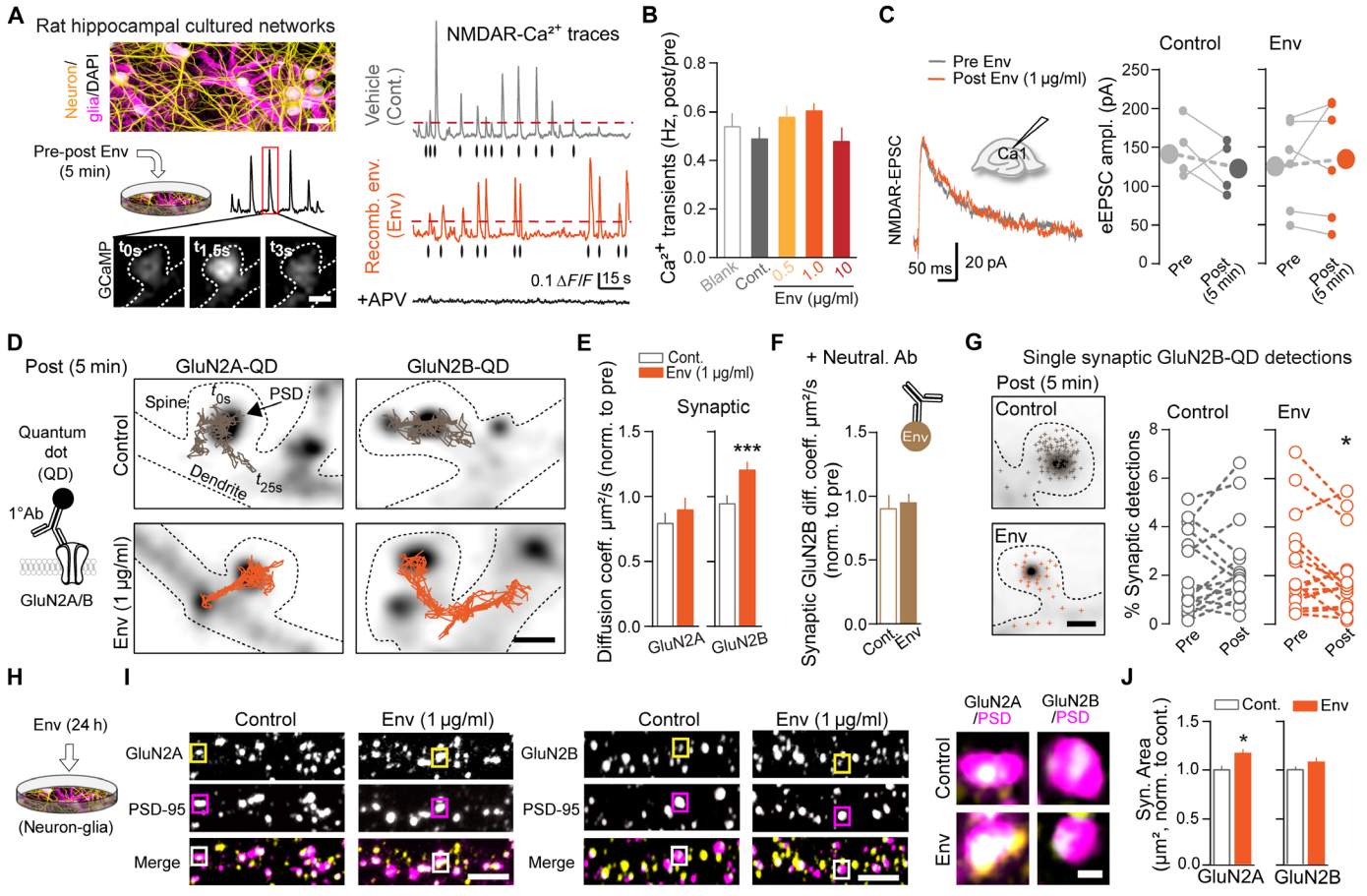

Fig. 1. Recombinant Env disperses synaptic NMDAR in hippocampal neurons without interfering with the ionotropic function. (**A**) Experimental setup of (yellow) neurons [microtubule-associated protein 2 (MAP-2) positive] and (magenta) glia [glial fibrillary acidic protein (GFAP) and Iba1 positive]. Representative NMDAR-mediated Ca^{2+} signals and detected transients (dots) 5 min after Cont. (vehicle) or Env exposure. Scale bars, 30 and 1 μm. (**B**) Ca^{2+} frequency ratio (post/pre) for blank (n = 47/5 spines/neurons); Cont. (n = 92/7); and Env: 0.5 μg/ml (n = 87/6), 1.0 μg/ml (n = 114/9), and 10 μg/ml (n = 18/1). (**C**) Representative NMDA traces and mean peak amplitudes before (pre) and 5 min after (post) Cont. or Env application. (**D**) Representative trajectories of GluN2A- and GluN2B-NMDAR-QD complexes at postsynaptic densities (PSD). Scale bar, 1 μm. (**E**) Synaptic increase of GluN2B-NMDAR but not GluN2A-NMDAR surface diffusion. Data are normalized to pre-exposure for individual neurons. GluN2A, Cont. (vehicle; n = 176/4 trajectories/neuron) and Env (n = 200/5). GluN2B, Cont. (n = 670/16) and Env (n = 792/17). ***P < 0.0001; Mann-Whitney tests. (**F**) Coapplication of Env-neutralizing Ab eliminates the Env effect, Cont. (n = 261/5) and Env (n = 490/5). (**G**) Paired data of synaptic GluN2B-QD complex detections from individual neurons (circles). *P = 0.037, paired Student's t tests. (**H**) Experimental setup. (**I**) Representative images of GluN2A-NMDAR and GluN2B-NMDAR (yellow) surface staining and their dendritic localization relative to postsynaptic areas (represented by PSD-95 staining). Right: Colocalized staining (white) count as synaptic NMDAR clusters. Scale bars, 4 and 0.5 μm. (**I** and **J**) Prolonged Env exposure specifically increases GluN2A synaptic cluster area in hippocampal neurons. GluN2A, Cont. (n = 28 neurons) and Env (n = 28); GluN2B, Cont. (n = 35) and Env (n = 35). *P = 0.031; Mann-Whitney tests. Dots are mean and bars are means ± SEM.

diffusion coefficient ± 25 to 75% interquartile range: **P = 0.0061, Mann-Whitney test) and increase NMDAR-mediated Ca^{2+} transient synchrony (Fig. 3F) in an IL-1R–dependent manner (Fig. 3F). Last, long-lasting changes in NMDAR surface dynamics have been shown to alter, through direct protein-protein interaction, the surface dynamics of dopamine D1 receptor (D1R) (*29*, *30*). After Env exposure (24 hours), the surface diffusion of D1R was significantly reduced (fig. S4, A and B), suggesting that Env disturbs both NMDAR surface organization and transmission and membrane partners such as the dopamine receptors.

On the basis of the changes in NMDAR-mediated activities, one may predict that the basal content of synaptic AMPA receptor (AMPAR) and the canonical NMDAR-dependent long-term plasticity of synapses will be altered in the presence of Env. To address this possibility, we first measured the effect of Env on the basal content of genetically expressed AMPAR. Env exposure (24 hours) increased the synaptic content of GluA1-AMPAR (Fig. 3, G and H). A short exposure to Env (5 min) was not sufficient to alter GluA1-AMPAR synaptic content [Cont., 1.0 ± 0.057, n = 45 neurons; Env, 0.89 ± 0.053, n = 48; means ± SEM; intensity (arbitrary units) normalized to control: P > 0.05], suggesting that the AMPAR synaptic potentiation builds up over time. To test whether the plastic range of synapses was affected, hippocampal networks were exposed to Env for 24 hours and then challenged by a chemically induced long-term potentiation protocol (cLTP) (*24*). cLTP was blocked by the NMDAR antagonist D-(−)-2-amino-5-phosphonopentanoic acid (APV) (not shown). After Env exposure, cLTP was abolished, with a marked decrease in AMPAR content (Fig. 3, I and J) that resembles a depotentiation of the Env-potentiated synapses (Fig. 3, G and H). Hence, Env tunes NMDAR network activity and basal and activity-dependent regulation of synaptic glutamate receptor content.

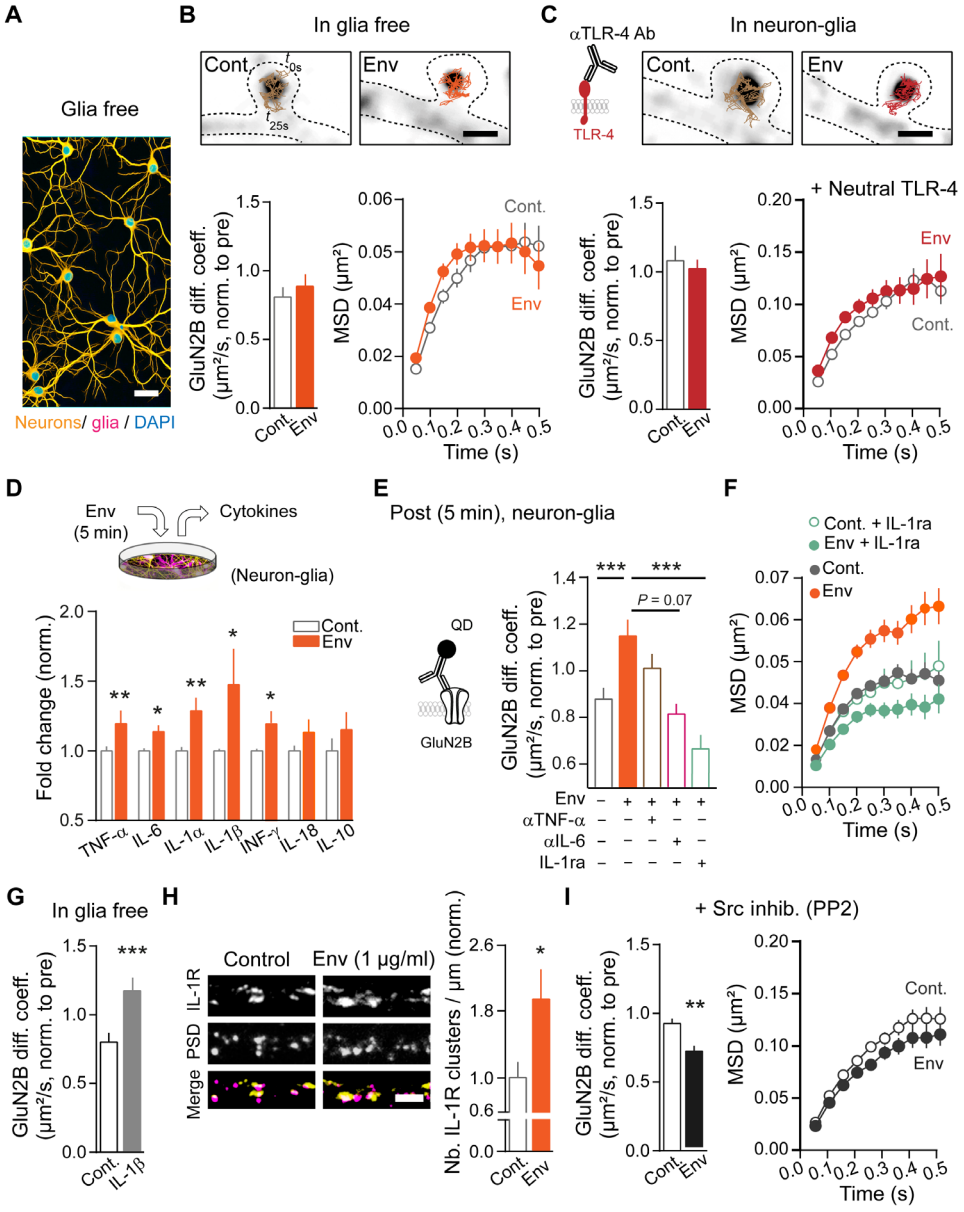

Fig. 2. Env laterally disperses synaptic NMDAR through glia-, TLR-4–, and cytokine-dependent processes. (**A**) Representative image of glia-free neuronal culture (yellow) neurons (MAP-2 positive) and (magenta) glia (GFAP and Iba1 positive). Scale bar, 50 μm. (**B**) GluN2B synaptic diffusion in glia-free cultures after 5-min vehicle (Cont., $n = 295/7$ trajectories/neurons) or Env (1 μg/ml; $n = 377/6$) exposure. (Right) MSDs. (**C**) GluN2B synaptic diffusion after Cont. or Env exposure in the presence of a TLR-4–neutralizing Ab. Cont. ($n = 163/5$) and Env (1 μg/ml; $n = 276/6$). (Right) MSDs. Scale bar, 1 μm. (**D**) Detected cytokine release in culture medium 5 min after Env (10 μg/ml) exposure, ($n = 5$ cultures) *$P = 0.037$, 0.026, and 0.026; **$P = 0.009$ and 0.009, paired Student's t tests. (**E** and **F**) GluN2B synaptic diffusion in the presence of Env (1 μg/ml) plus αTNF-α, αIL-6 (1 μg/ml) blocking Ab's or IL-1ra (250 ng/ml). Cont. (vehicle; $n = 579/6$), Env ($n = 352/6$), Env + αTNF-α ($n = 461/5$), Env + αIL-6 ($n = 404/4$), and Env + IL-1ra ($n = 365/7$). ***$P < 0.0001$ and 0.006, Kruskal-Wallis test followed by Dunn's multiple comparisons. (F) MSDs for data in (E) including Cont. + IL-1ra ($n = 176/7$). (**G**) Increased GluN2B surface diffusion after 5 min of IL-1β exposure in glia-free hippocampal cultures. Cont. ($n = 423/7$) and IL-1β (1 ng/ml; $n = 480/7$). ***$P < 0.0001$, Mann-Whitney test. (**H**) Representative images of IL-1R (yellow in merge) staining and their dendritic localization relative to postsynaptic areas (represented by PSD-95 staining; magenta in merge). Scale bar, 5 μm. (Right) Env exposure rapidly (5-min range) increases IL-1R cluster number on dendrites. Cont. ($n = 55$ dendrites) and Env ($n = 51$). *$P = 0.019$, Mann-Whitney test. (**I**) GluN2B synaptic diffusion after Cont. or Env exposure in the presence of a Src family inhibitor (PP2; 1 μM). Cont. ($n = 743/6$) and Env (1 μg/ml; $n = 492/6$); **$P = 0.0031$, Student's t test. (Right) MSDs. Data (means ± SEM) are normalized to pre-exposure for individual neurons.

Env expression in the rat hippocampus triggers behavioral deficits

Alterations of NMDAR signaling and synaptic plasticity often generate behavioral deficits, some of which are commonly related to models of psychosis (*31*). Therefore, we investigated whether Env expression in the developing rat hippocampus alters adult behavior. For this, Env gene was expressed in hippocampal neurons and astrocyte/radial glial cells by postnatal electroporation (Fig. 4, A and B, and fig. S5A). Most electroporated cells were found in CA regions of the hippocampus, with only few cells in the dentate gyrus

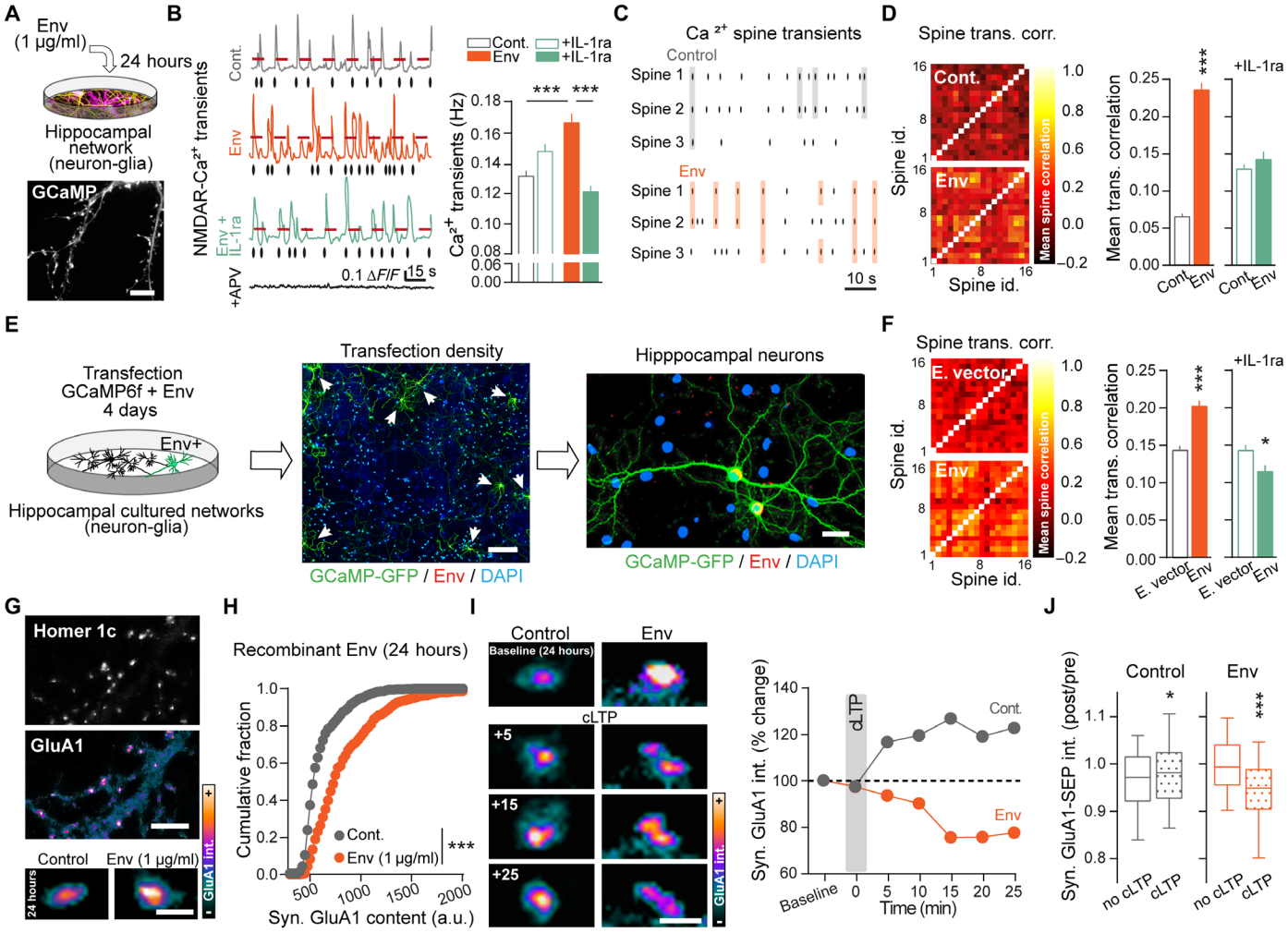

Fig. 3. Prolonged Env exposure potentiates glutamatergic synapse transmission and prevents long-term potentiation. (**A**) Experimental setup. Scale bar, 10 µm. (**B**) Representative NMDAR-mediated Ca^{2+} signals and transients (dots). Increased Ca^{2+} transient frequency after 24 hours of Env exposure is reversed by IL-1ra (250 ng/ml). Cont. (vehicle; n = 88/8 spines/neurons), Cont. + IL-1ra (n = 115/7), Env (n = 73/10), and Env + IL-1ra (n = 101/7). ***P = 0.0001, two-way analysis of variance (ANOVA), Bonferroni's multiple comparisons. (**C**) Ca^{2+} transient detections (dots) and correlated timing (shaded areas) from spines on representative neurons exposed to Cont. or Env. (**D**) Characteristic correlograms of mean spine transients and (right) quantitative shuffle corrected graphs. ***P < 0.0001, Mann-Whitney tests. (**E**) Experimental setup and representative images of cotransfected neurons, density ~ 3%. Scale bars, 300 and 40 µm. (**F**) Correlograms and quantitative shuffle corrected graphs from Cont. (empty vector) and Env (phCMV-MSRV Env) transfected cells in combination or not with IL-1ra. E. vector (n = 126/8), E. vector + IL-1ra (n = 114/8), Env (n = 159/8), and Env + IL-1ra (n = 139/8); ***P < 0.0001 and *P = 0.026, Mann-Whitney tests. (**G**) Live surface GluA1 expression in synaptic areas (Homer 1c). Scale bars, 5 and 1 µm. (G below and **H**) Synaptic GluA1 fluorescence intensity after 24 hours of Env exposure, Cont. (vehicle; n = 1071/25 spines/neurons), and Env (n = 728/21). ***P < 0.0001, Kolmogorov-Smirnov test. (**I**) Live time-lapse images of representative spines at baseline (−5 min) and after chemical LTP (cLTP) induction and (right) example of GluA1 fluorescence dynamics, normalized to baseline. Scale bar, 1 µm. (**J**) GluA1 intensity ratio between baseline (pre, mean: −10 and −5 min) and post-cLTP (mean: 20 and 25 min) for individual spines. Cont., no cLTP (n = 621/13 spines/neurons) and cLTP (n = 902/12); and Env, no cLTP (n = 461/17) and cLTP (n = 472/14). *P = 0.023 and ***P < 0.0001, Mann-Whitney tests, box-and-whisker plot (10th to 90th percentile). Data represent means ± SEM unless mentioned otherwise.

(Fig. 4A). Immunostaining against Env confirmed its cellular expression (Fig. 4B). There was no evidence of cellular toxicity at P7, as evaluated by a cell death marker (fig. S5, B and C), and myelin basic protein staining did not reveal any overall effect on myelin integrity at ~P65 (fig. S5D), and the body weight of control and Env electroporated animals was similar (fig. S6A). To determine whether Env triggers inflammation, microglia cells were immunostained (fig. S5E). Env expression increased the microglia density [Cont., 155 ± 10, n = 16 hippocampi; Env, 210 ± 13, n = 20; means ± SEM (cells/mm^2): **P = 0.0019] and the percentage of Iba1-positive cells at P7 but not at P65 (fig. S5, E and F). Thus, Env was successfully expressed in the developing hippocampus in which it triggers an expected activation of microglia cells.

Using a sequence of behavioral tests, we report that control and Env rats exhibited similar novelty-induced and adapted locomotion, without behavioral signs of anxiety (Fig. 4, C and D, and fig. S6B). However, Env rats had exaggerated sensitivity to a single injection of the psychotomimetic drug, MK-801 (NMDAR channel blocker) (Fig. 4E). Their performance in the social recognition test was hampered (Fig. 4, F and G), suggesting an impaired working memory and/or increased social or preservative behaviors. Yet, the level of social interactions (time of active engagement) was undisguisable

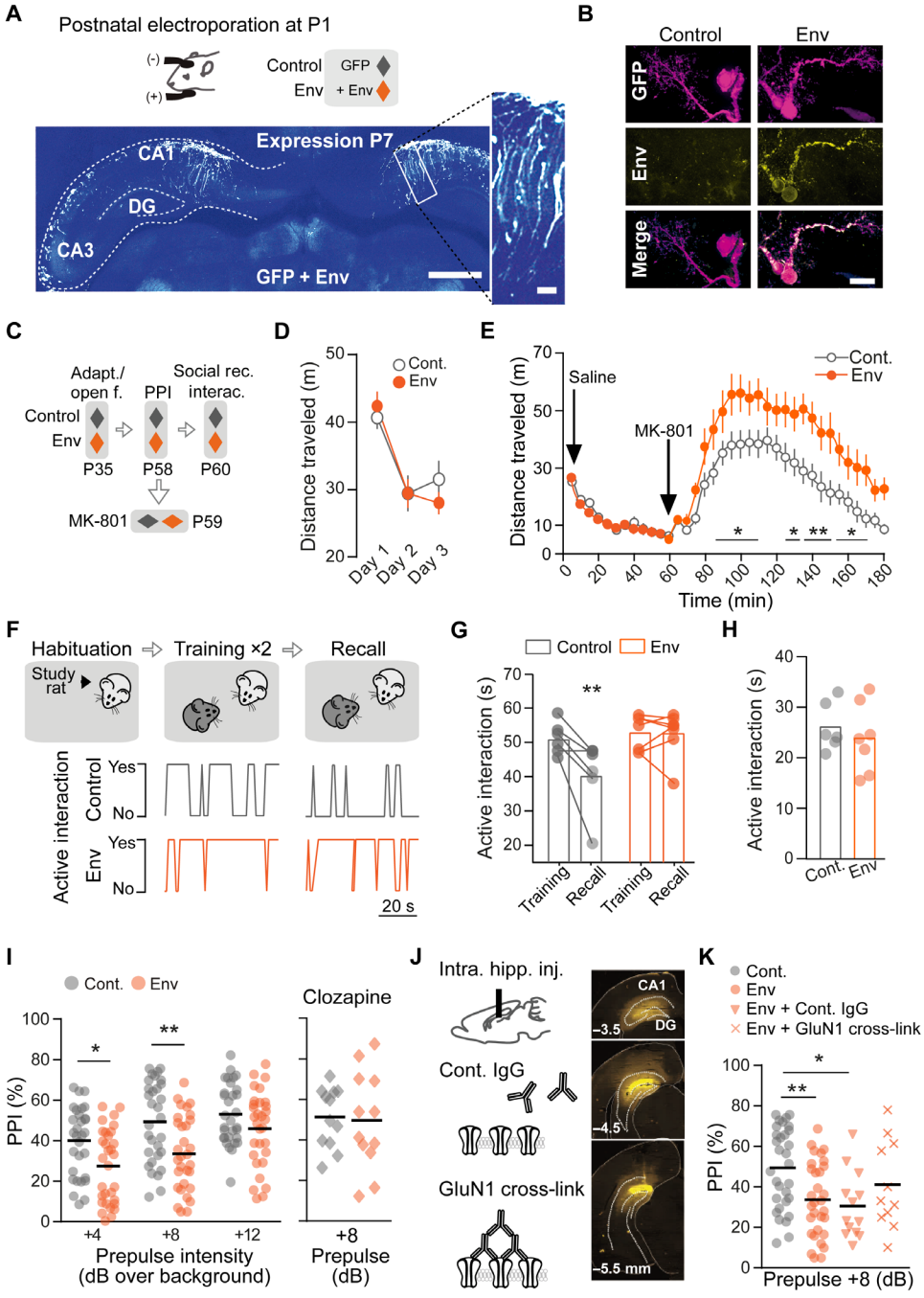

Fig. 4. Env expression in rat hippocampus triggers behavioral deficits that are prevented by an antipsychotic or reduced by NMDAR surface stabilization. (**A**) Electroporation at postnatal day (P)1. Representative images of hippocampal inserted gene distribution. Scale bars, 1 mm, and inset, 100 μm. (**B**) Env-expressing cell from the CA1 region at P7. Scale bar, 40 μm. (**C**) Behavioral study sequence: adaptation (adapt.)/open field, prepulse inhibition (PPI), followed by social recall and interaction or NMDAR antagonist (MK-801) challenge. (**D**) Basal locomotion and adaptation to context measured as distance traveled (m) during 20 min ($n = 12$), means ± SEM. (**E**) MK-801 (0.3 mg/kg) induced hyperlocomotion; $^*P < 0.05$ and $^{**}P < 0.01$, RM two-way ANOVA, Fisher's least significant difference (LSD) post hoc analysis ($n = 9$ to 11), means ± SEM. (**F**) Social recognition protocol. (Bottom) Representative scored interaction (Yes or No, during 1 min) at training and recall sessions; ITI, 3 min. (**G**) Env animals show constant levels of interaction with a familiar rat. $^{**}P = 0.005$; Trial factor: $F(1,11) = 8.27$, two-way RM ANOVA and Sidak's multiple comparisons test ($n = 6$ to 7). (**H**) Social interaction measurements are similar in control and Env rats ($n = 6$ to 7). (**I**) Env impairs PPI startle response. $^*P = 0.018$ and $^{**}P = 0.002$, Group factor: $F(1,180) = 20.46$; $^{***}P < 0.0001$, two-way ANOVA, Bonferroni's multiple comparisons test, ($n = 31$). (Right) Clozapine (12 mg/kg) induced recovery. (**J**) Illustration of cross-link protocol. (Right) Representative intrahippocampal injection site. (**K**) PPI response in Env animals after GluN1 cross-link compared to control animals ($P = 0.5970$) (I) from parallel experiments. $^*P = 0.0195$ and $^{**}P = 0.0093$; one-way ANOVA corrected for unweighted means and Tukey's multiple comparison test. Dots are individual animals, and bars/lines represent means.

between control and Env rats (Fig. 4H). Env rats responded poorly to the prepulse inhibition test (PPI) test (Fig. 4I and fig. S6C) with similar startle amplitudes when compared to control rats. These results indicate that Env expression in the hippocampus is sufficient to trigger behavioral deficits associated with psychosis. Consistently, the antipsychotic drug, clozapine, prevented the PPI test alterations in Env rats (Fig. 4I, right, and fig. S6D). Because Env induced NMDAR dysfunctions through their lateral dispersion, we artificially stabilized surface NMDAR in the hippocampus of Env-expressing rats using a GluN1 cross-link protocol before testing their PPI response (Fig. 4J) (*24*). The artificial stabilization of surface NMDAR improved the PPI responses of Env rats, as there were differences between control and Env, as well as control and Env + control immunoglobulin G (IgG) but no significant difference between control and Env + GluN1 cross-link ($P = 0.5970$) (Fig. 4K and fig. S6E). Collectively, these data indicate that Env expression in the developing hippocampus is sufficient to induce behavioral deficits associated with psychosis in adults, most likely through an altered NMDAR membrane dynamics.

Neonatal Env expression tunes glutamatergic synapse maturation and induces behavioral deficits associated with psychosis

The proper maturation of glutamatergic synapses requires a switch from immature GluN2B-rich to mature GluN2A-rich synapses (*19*). This fundamental process occurs during the postnatal period (first two postnatal weeks) in which neuronal networks and cognitive functions are established. Synaptic alterations occurring during this time window often lead to adult behavioral dysfunctions associated with psychiatric disorders, such as psychosis (*19*, *32*, *33*). Considering that the GluN2A/2B synaptic ratio was altered in vitro by Env, we measured the GluN2A- and GluN2B-NMDAR synaptic content (Fig. 5A and fig. S7, A to C) at the end of the first postnatal week (P7) and at adult stages (>P65). At these stages, inserted genes were clearly present in hippocampal areas, as observed by immunohistochemical and biochemical means (Fig. 5, B and C). The GluN2A-NMDAR synaptic content increased over development, whereas GluN2B-NMDAR content decreased (Fig. 5, D and E). However, in Env rats, the GluN2A-NMDAR synaptic content was already increased at P7 ($P = 0.06$), which flattens the following developmental rise from P7 to P65 (Fig. 5D). The GluN2B-NMDAR synaptic content remained stable in Env rats compared to control rats at both ages (Fig. 5E). The relative amount of GluN2A-NMDAR and GluN2B-NMDAR at the adult stage was thus consistently decreased (Cont., 1.0 ± 0.08; Env, 0.90 ± 0.10, $n = 8$; means ± SEM: $^*P = 0.034$; Student's t test). Since there was a clear sign of inflammation at P7 (Fig. S5, E and F), we tested whether a change in the interaction between IL-1 and GluN2A-NMDA receptors (*34*) could explain the early alteration in synaptic NMDAR. The co-IP (immunoprecipitation) between GluN2A-NMDAR and IL-1R was significantly increased in Env-hippocampal synapses at P7 (Fig. 5F), whereas the co-IP between GluN2B-NMDAR and IL-1R was unaffected. At the adult stage, there was no significant difference in all groups (GluN2A/IL-1R: Cont.: 1.0 ± 0.15, Env: 1.04 ± 0.21; GluN2B/IL-1R: Cont.: 1.0 ± 0.08, Env: 0.95 ± 0.09, $n = 6$ to 7; means ± SEM; $P > 0.05$). Because Env potentiated AMPAR synaptic content in cultured hippocampal networks (Fig. 3, G and H), we lastly compared the AMPAR synaptic content at adult stages (at P7, the vast majority of glutamatergic synapses lack AMPAR). The synaptic content was significantly increased in Env rats when compared to control ones (Fig. 5G and fig. S7D). The overall amount of PSD-95 was unaltered in Env rats (Fig. 5H). Thus, the neonate expression of Env alters the developmental maturation of NMDAR subtypes with a premature increase in synaptic GluN2A-NMDAR driven by a functional interplay with the IL-1R signaling complex. This accelerated maturation in NMDAR signaling potentiates glutamate synapses at a later stage, likely impairing their plastic window.

Because the maturation of glutamatergic synapses occurs during the first postnatal weeks, we postulated that the deleterious effect of Env on the NMDAR signaling and synapse maturation is prominent during this period. To test this hypothesis, Env rats received injections of Env-neutralizing antibody from P4 to P12 (three injections; Fig. 5I). At the adult stage, while the Env-induced PPI deficit was still observed in rats that received the control antibody, the behavioral response was clearly restored by Env-neutralizing antibody treatment (Fig. 5J and fig. S7, E and F). These data indicate that Env expression in the early postnatal period alters the synaptic GluN2A/B-NMDAR maturation and drives the emergence of behavioral abnormalities in adults.

HERV Env from sera of patients with psychosis alters NMDAR surface organization

A substantial fraction of patients diagnosed with schizophrenia or bipolar disorders express HERV-W Env (*10*–*12*). To test whether the HERV Env from patients diagnosed with psychosis has the capacity to alter neurotransmitter systems, including the NMDAR, sera from Env-negative and Env-positive subjects were collected and compared. First, a higher level of the proinflammatory cytokine, IL-1β, was detected in Env-positive samples (fig. S8, A and B, and table S1), whereas the levels of other cytokines and inflammatory markers (e.g., C-reactive protein) remain unchanged. Tagged AMPAR, NMDAR, D1R, or inhibitory γ-aminobutyric acid (GABA) type A receptors were expressed in hippocampal neurons that were briefly exposed to sera from Env-negative and Env-positive subjects. After tens of minutes, the surface clusters of tagged receptor were examined in live cells (fig. S8, C to E). We report that NMDAR surface clusters were altered in Env-positive sera, whereas none of the other neurotransmitter receptor content was significantly altered (fig. S8E). Thus, the serum of patients with psychosis that express Env is able to acutely disorganize surface NMDAR.

DISCUSSION

In this study, we provide direct evidence that the retroviral HERV-W Env protein, which is normally silenced but present in the sera of patients with psychosis (*10*–*12*), profoundly disturbs the maturation of hippocampal glutamatergic synapses and induces behavioral deficits associated with psychosis in the adult rat. At the molecular level, Env alters the synaptic content and trafficking of NMDAR through TLR-4–expressing glial cells and cytokines. It thus appears that the expression of HERV-W Env in the neonate hippocampus is sufficient to corrupt the establishment of neuronal networks. This also provides unexpected evidence that a product from a mobile genetic element, HERV, directly disturbs the canonical NMDAR-dependent maturation of excitatory synapses through immune-related molecules, supporting the view that a dysfunctional interplay between genetic, synaptic, and immune pathways may contribute to the etiology of psychotic disorders.

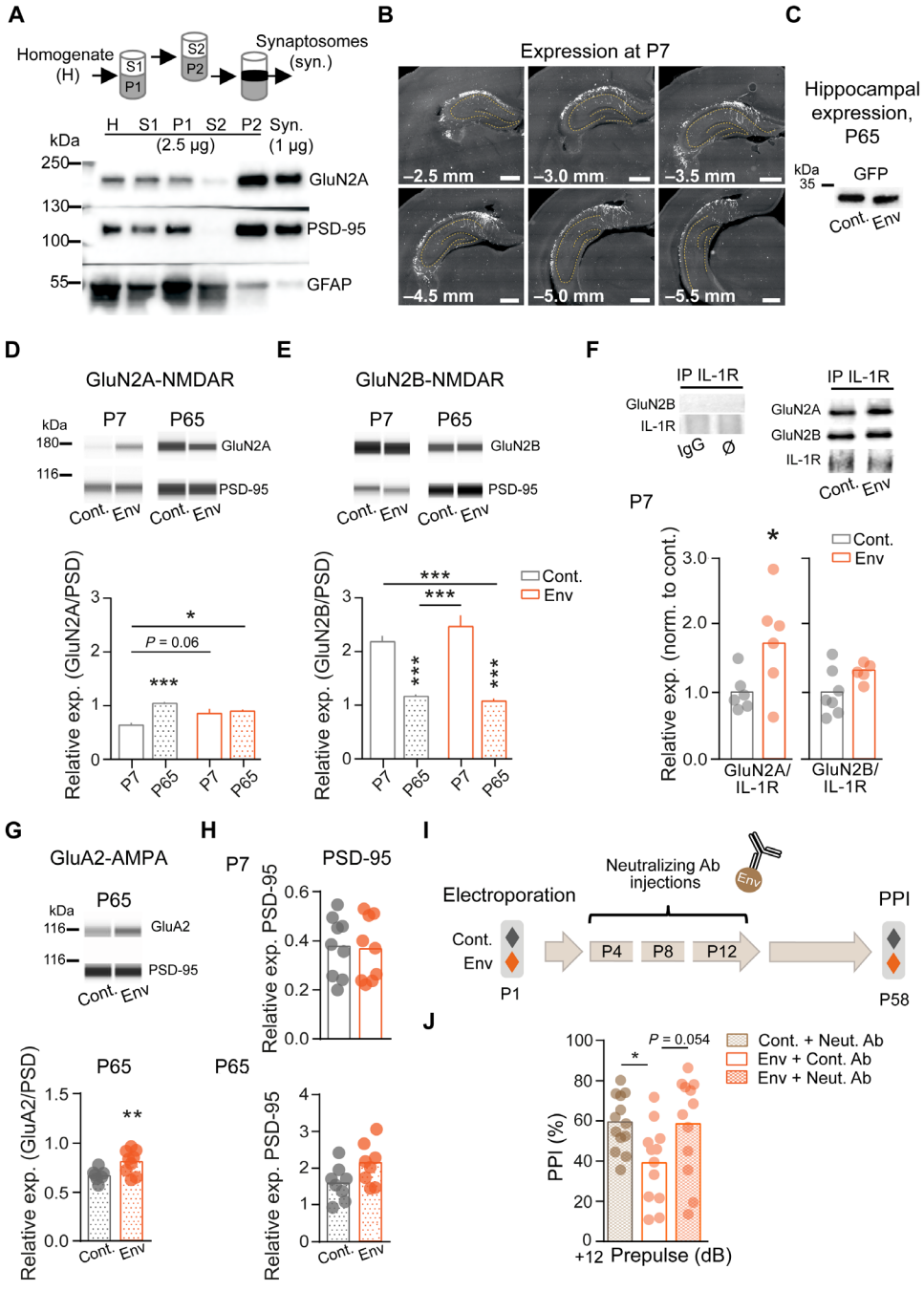

Fig. 5. Neonatal Env expression tunes glutamatergic synapse maturation and is necessary for psychotic-like behavior. (**A**) Subcellular fractionation of hippocampal tissue. Note the enrichment of NMDA receptors (represented by GluN2A) and postsynaptic density proteins (PSD-95) in P2 and synaptosome (synaptic proteins enriched) fractions compared to initial homogenate and the depletion of glia (GFAP) in the same. (**B**) Representative images of inserted gene distribution at P7. Scale bars, 1 mm. (**C**) Hippocampal inserted gene expression at ~P65. (**D**) Env exposure tends to influence GluN2A/PSD-95 subunit stabilization in the synapse (P7; Cont. versus Env; $P = 0.06$) that then remains constant. Interaction: $F(1,29) = 8.69$, two-way ANOVA and Bonferroni's multiple comparisons test; $^{*}P = 0.021$ and $^{***}P = 0.0004$. (**E**) GluN2B/PSD-95 expression is unaffected by Env at both ages. Interaction: $F(1,29) = 2.46$, $P = 0.13$, two-way ANOVA and Bonferroni's multiple comparisons test; $^{***}P < 0.0001$ ($n = 8$ to 9 animals per group). Bars are means ± SEM. (**F**) At P7, Env animals exhibit increased GluN2A–IL-1R interactions. Immunoprecipitation (IP) of IL-1R. $^{*}P = 0.0462$, Student's t test ($n = 5$ to 7 animals per group). Ø, nothing. (**G**) GluA2/PSD-95 expression is increased in adult animals. $^{**}P = 0.0098$, Students t test ($n = 6$ to 9 animals per group). (**H**) PSD-95 expression is similar comparing Cont. and Env from both P7 and P65 rats. (**I**) Early postnatal treatment protocol (intraperitoneal injections) at P4, P8, and P12 with an Env-neutralizing Ab (30 mg/kg). (**J**) Treatment improves Env animals' PPI responses. $^{*}P = 0.037$, one-way ANOVA and Tukey's multiple comparison test. Dots are individual animals and bars represent means.

At hippocampal CA1 glutamate synapses, the postsynaptic maturation is characterized by various molecular changes including GluN2A/B subunit switch, protein kinase recruitment, and AMPAR incorporation/stabilization (*19*). The developmental change in NMDAR subunit composition has been under high scrutiny since it affects synaptic plasticity and plays a key role in the maturation of forebrain synapses and neuronal networks. This highly sensitive process that relies on neuronal activity and sensory experience is likely corrupted in neurodevelopmental psychiatric disorders (*18*, *19*). Here, we provide direct evidence that the expression of Env during development alters the GluN2A/2B ratio in maturing synapses, through destabilization and lateral escape of membrane GluN2B-NMDAR, leading to deficits in synaptic plasticity and behavior. This is consistent with the impaired long-term synaptic plasticity and associative memory functions after artificial alteration of NMDAR membrane dynamics in the developing hippocampus (*24*, *35*). Furthermore, the Env-induced change in GluN2B-NMDAR trafficking increased the relative 2A/2B synaptic ratio already during early development, which likely translates to a premature development of the glutamate synapses affecting their adaptations (as witnessed by the AMPAR synaptic potentiation). Although Env from various HERV families can have toxic effects on specific cell types (*3*, *10*, *26*), our data show that HERV-W Env is not cytotoxic per se for hippocampal neurons and glial cells. Moreover, the altered NMDAR expression following neuronal exposure to human Env-positive serum samples further supports a glutamatergic imbalance related to Env. Noteworthy, although the dose of purified Env protein used here in vitro was higher than the ones measured in patients' sera, the gene expression of HERV-W Env in brain cells was sufficient to reproduce the effects and provide similar Env immune labeling as the one reported in patients' tissue (*36*), suggesting that the Env concentrations used in the study are within the active range of action. Together, our data support a model in which early-life expression of the HERV protein, Env, accelerates the maturation of NMDAR signaling and glutamatergic synapses, altering the critical postnatal period for synaptic and network maturation.

Contrary to the classical psychotomimetic drugs that are potent NMDAR antagonists (*18*), Env did not act as a receptor antagonist. Instead, the NMDAR synaptic dysfunction, i.e., lateral translocation, was mediated by a glial-, TLR-4–, and cytokine-mediated process, consistent with the emerging role of glial cells in the etiology of neuropsychiatric disorders, such as schizophrenia (*16*, *17*). Indeed, microglial activation, observed in animal models of psychosis and patients with schizophrenia, accelerates synaptic development through excessive synaptic pruning (*16*, *17*). Beside complement factors, microglia release proinflammatory cytokines, which are up-regulated in patients with psychotic disorders (*37*). On the basis of our observation that IL-1R is essential to mediate the Env effects on NMDAR functions, we propose a model in which IL-1R rapidly tunes the membrane trafficking of GluN2B-NMDAR. This is likely achieved through the activation of intracellular cascades with Src kinases and the formation of membrane IL-1R/NMDAR complexes that can be regulated by the GluN2B subunit phosphorylation following IL-1R activation (*34*, *38*). Thus, it emerges that HERV-W Env alters the maturation, and possibly pruning, of glutamatergic synapses through the activation of microglial cells and release of cytokines.

Various types of HERV Env exist, and future investigations are surely needed to clarify their origin and convergence of actions (*3*). In multiple sclerosis, HERV-W expression essentially takes place in the central nervous system in microglial cells and may also be expressed by few infiltrated B cells and macrophages (*36*). Furthermore, the Env of HERV-K type has also been detected in patients with ALS, and its pathogeny is demonstrated through impairment of glutamatergic synaptic transmission and progressive motor behavior deficits (*10*). The canonical glycoprotein (gp)120, which is an Env protein derived from the exogenous HIV-1, has been related to the HIV-associated neurocognitive disorders found in many patients with HIV (*39*). In the brain, gp120 increases NMDAR-dependent glutamatergic transmission and potentiates glutamate-induced increase of intracellular calcium concentrations (*40*). Consistent with our study, gp120 essentially targets GluN2B-NMDAR transmission, involving phosphorylation changes following glial cell activation and IL-1β release (*40*). These studies thus underline the growing body of evidence for an etiological role of Env proteins in major neurological and psychiatric disorders (*3*, *9*). Noteworthy, although we and others provide direct evidence that Env itself can induce deficits in synaptic functions and behavior, a role of the other HERV gene products (e.g., the *gag* protein) remains a possibility to be thoroughly explored. For instance, the activity-regulated cytoskeleton-associated protein Arc (also known as Arg3.1), which is a potent regulator of the glutamatergic synapse transmission (*4*, *6*), is of retroviral origin with clear homology to *gag* proteins. Consistent with such retroviral origin, it has been proposed that Arc mediates its action across synapses through exovesicles (*5*, *41*). Since Arc dysfunctions have been associated with neuropsychiatric illnesses [e.g., de novo mutation observed in patients with psychotic disorders (*32*)], the possibility that, in addition to Env, other HERV products or proteins with ancient retroviral origin contribute to the deficit in brain cell communication and network physiology in psychiatric disorders emerges as a new conceptual framework.

At the translational level, one key challenge will be to define the trigger of HERV activation. It has long been proposed that chronic infection and/or infections during specific developmental periods (e.g., influenza virus during pregnancy) are associated with an increased risk to develop psychotic disorders (*42*). The HERV-W gene activation found in patients with neuropsychiatric disorders (*11*–*13*) likely originates from a perinatal infection that is followed by a secondary environmental insult (*14*). Our data support a model in which the developmental expression of the HERV-W gene product (Env) profoundly alters the maturation of glutamatergic synapses and network organization. This suggests that Env plays a key role in the developmental emergence of behavioral dysfunctions associated with psychosis at adult stages. Because immune challenges are a known activator of HERV genes, HERV may have a place as a biological substrate of the canonical genetic and environmental interplay at the basis of psychotic disorders. Ongoing clinical trials that aim at neutralizing Env will likely raise immense hope to treat HERV Env-positive patients with neuropsychiatric conditions.

MATERIALS AND METHODS

Study design

We designed this study to determine whether HERV-W–derived Env protein could play a role in the known glutamatergic, namely, NMDAR, disturbance of developmental neuropsychiatric disorders. We first showed that the ionotropic function of the receptor (NMDAR antagonists are related to psychotic-like effects) was intact after Env exposure and that, instead, the surface diffusion of the NMDAR-GluN2B

subtype was sensible to Env. The recombinant Env buffer was used as control, and in addition, heat inactivation and neutralization with a specific Env antibody proved Env's involvement. At the start of single-particle tracking experiments, the sample size was, on the one hand, determined by referring to previous studies from the laboratory (*24*) and, on the other hand, calculated (Power and Sample Size Calculator, Statistical Solutions LLC) with a power factor of 0.6 to 0.8 and α of 0.5, which, in our condition, was translated to 4 to 13 cells per condition depending on the SD of the sample. For all types of experiments, a minimum of three independent cultures were used per condition. Cultures were chosen at random and experimental conditions were alternated throughout the live imaging experiments; the experimenter was blind to the condition during removal of unspecific trajectories while all other analyses were done on a fully automated basis. Immunocytochemistry showed that the expression of the important synaptic GluN2A/2B-NMDAR subunit balance was affected. All analyses involving immunohistochemistry/immunocytochemistry were performed blindly. We ensured that no toxicity was induced by Env in our neuronal networks by adding propidium iodide and visualizing healthy cell bodies after Env exposure. We next measured the global NMDAR-mediated activity, as well as NMDAR-dependent LTP, and observed an increase in calcium frequency and ablation of cLTP induction in the Env-treated cultures. In the chemical LTP experiments, a variation above 10% of GluA1-Super Ecliptic pHluorin (SEP) intensity in single synapses during baseline was considered as unstable and, hence, this spine was excluded; for calcium imaging, spines with more than two calcium bursts after D-APV application were considered as non-NMDAR and excluded. We then transfected neuronal cultures with a plasmid containing the HERV-W Env and observed similar results. A plasmid with an empty vector was used as control.

We then asked whether specific Env expression could affect an animal's behavior. For this, we expressed the Env in the hippocampus of rat pups from postnatal day 0 and studied its impact on a series of behavioral studies. We controlled for cellular toxicity by evaluating terminal deocynucleotidyl transferase–mediated deoxyuridine triphosphate nick end labeling (TUNEL)–stained cells and weight gain of the animals, and the presence and extent of Env expression were confirmed by immunohistochemistry and Western blot analysis. Expression of GFP and additionally an empty vector was used in control animals. For behavioral studies, the predetermined minimum sample size of 12 animals was based on previous studies. In our hands, a sample size of 13 to 18 animals in PPI was used, which corresponded to a power factor of 0.6 to 0.75 and α of 0.5, and in the x-link and MK-801 experiments, a sample size of 11 animals corresponded to a power factor of 0.55 and <0.8, respectively. Rat pups from the same litter were assigned to different experimental groups in a randomized manner, and groups were pseudorandomized on each behavioral testing day. As predetermined, potentiation of PPI in response to prepulses and stereotypic behavior in the MK-801 challenge test were used as exclusion criteria. During animal studies, the experimenter was not blind to the animal's condition since all analyses were done on a fully automated basis at the end of the experiment, after collecting the complete dataset. As we observed deficits in several behavioral tests, we then investigated the animal's hippocampal NMDAR expression to relate our in vitro data to a possible underlying cause for these observations. Protein expression studies were conducted with nine animals per condition and replicated two to three times. By specifically neutralizing the Env during development, we observed a clear improvement of the behavioral response. The data showed that HERV-W Env expression in the hippocampus induces behavioral deficits and modulates the synaptic NMDAR maturation during development.

Expression of the Env in serum from seven patients with neuropsychiatric disorders was detected by enzyme-linked immunosorbent assay. Serum samples from six individuals with no known brain disease were used as controls, and sample sizes were based on the availability of samples. In a pilot experiment, we stimulated neuronal networks transfected with plasmids containing the main neurotransmitter receptors (AMPA, NMDA, dopamine, and GABA) with our serum samples and observed that Env-containing serum specifically induced NMDAR alterations. Full description of all data can be found in table S2.

Env protein

Recombinant Env [full-length multiple sclerosis-associated retrovirus (MSRV) Env protein of 548 amino acids; Env pV14; GenBank accession no. AF331500] was produced by PX'Therapeutics (Grenoble, France) according to the quality control specifications of GeNeuro (Geneva, Switzerland). Endotoxin removal was done by polishing batches through Mustang Q Acrodisc followed by filtration on a 0.22-μm filter (Stericup; Merck, Darmstadt, Germany). Endotoxin levels for Env batches used were between 13.6 and 92.3 endotoxin units/ml, as measured by the limulus amebocyte lysate test. Influence of endotoxin on our results was excluded by observations after heat inactivation, 100°C for 30 min, as previously described (*26*).

Receptor surface diffusion experiments

Neurons were transfected with the postsynaptic marker Homer 1c–DsRed at 7 days in vitro (div). High-resolution single molecular tracking of NMDARs was achieved after 10 min of incubation at 37°C with antibodies against extracellular epitopes of either the GluN2A or the GluN2B subunits (Alomone Labs, Jerusalem, Israel; table S3) at 11 to 14 div. After 10 min of incubation with quantum dots 655 (Invitrogen, Thermo Fisher Scientific, Massachusetts, USA) in medium with 1% bovine serum albumin (Sigma-Aldrich, Missouri, USA), selected regions of interest (ROIs) (with Homer 1c–expressing neurons) were imaged for 500 consecutive frames with an acquisition time of 50 ms on a Nikon eclipse T*i* epifluorescent microscope using an electron-multiplying charge-coupled device (EMCCD) camera (Evolve; Photometric, Tuscon, USA). Acquisition was made with MetaMorph software (version 7.7.11.0; Molecular Devices, Sunnyvale, USA). The instantaneous diffusion coefficient (D) was calculated for each trajectory from linear fits of the first four points of the MSD versus time function using $\mathrm{MSD}(t) = (r^2)\,(t) = 4Dt$. To determine the distribution of single QD complexes, frame stacks were obtained, and after the binarization of the synaptic signal, the complexes were automatically located into synaptic (Homer 1c–positive area including the surrounding two pixels) and extrasynaptic compartments. The percentages of synaptic locations per stack in relation to the total amount were calculated, and the two highest deltas (pre-post) were excluded as outliers from each group. Data were projected on a single background image, providing high-resolution distribution of receptor/QD complexes and their trajectories. All single-particle analysis was completed using the PALMTracer version 1.0 plugin in MetaMorph software (Molecular Devices). The effect of Env (GeNeuro) or LPS (Sigma-Aldrich) compared to respective vehicle (controls) on receptor surface diffusion was

addressed using two approaches: (i) after 5 min of bath application in the imaging chamber following an initial baseline acquisition or (ii) 24 hours after protein application to the culture medium in the dish. Recombinant IL-1β (R&D Systems, Minnesota, USA) was only evaluated after 5 min of application. TLR-4 involvement was studied by blocking the receptor through preincubation for 30 min with an anti–TLR-4–neutralizing antibody (20 μg/ml; Affymetrix, Wien, Austria) at 37°C before onset of QD experiment. The specificity of the TLR-4–neutralizing antibody was confirmed by principal TLR-4 staining on Iba1-positive microglia cells (fig. S2A) and decreased staining after shTLR-4 transfection (plasmid kindly provided by P. Küry; fig. S2B). To confirm the specificity of our Env results, on the one hand, heat inactivation of the protein was performed (see above) and, on the other hand, preincubation of the recombinant Env protein with Env-neutralizing antibody, GN_ENV_01/03 (GeNeuro), in normal horse serum at a molecular weight ratio (1:2) was performed in glass tubes for 45 min at room temperature before application. For isolation of a postsynaptic response, TTX (1 μM; Tocris, Bristol, UK) was applied into the chamber before recordings, and for cytokine blocking experiments, IL-1ra (250 ng/ml; R&D Systems) or the neutralizing antibodies IL-6 and TNF-α (1 μg/ml, R&D Systems) were applied into the chamber before recording sessions. The involvement of Src family kinases was evaluated after 15 min of incubation with 1 μM PP2 (Calbiochem, Merck).

Calcium imaging

Neurons transfected with GCaMP3 or GCaMP6 at 10 div were transferred into Tyrode's solution containing 110 mM NaCl, 5 mM KCl, 25 mM Hepes, 15 mM D-glucose, 2 mM $CaCl_2$, and 2 mM $MgCl_2$. For isolation of NMDAR-dependent transients, the neurons were then moved to Mg^{2+}-free Tyrode's solution with 5 μM nifedipine (Tocris) and 5 μM bicuculline (Tocris) 15 min before imaging. Time-lapse images were acquired with MetaMorph software (Molecular Devices) at 20 Hz on a Nikon eclipse T*i* epifluorescent microscope with an EMCCD camera (Evolve, Photometric). To assess immediate effects, three time-lapse movies (3000 frames) were successively recorded: pre (baseline), post [5 min after bath application of phosphate-buffered saline (PBS) (blank), vehicle (control), or Env], and APV [5 min after 50 μM APV (Tocris) bath application]. For prolonged effects, two time-lapse movies were recorded: first, 24 hours after vehicle (control), Env (1 μg/ml), vehicle + IL-ra (250 ng/ml), or Env + IL-ra addition, or 4 days after transfection with the Env gene or an empty vector, and second, 5 min after APV bath application. Time-lapse movies were concatenated and realigned in ImageJ [National Institutes of Health (NIH)] with the PoorMan3DReg plugin (M. Liebling). Fluorescence from calcium transients versus time was measured within individual ROIs (spines) manually defined by the experimenter (ImageJ, NIH). All pixels within each ROI were averaged to give a single time course associated with the ROI. Mean normalized fluorescence ($\Delta F/F$) was calculated by subtracting each value with the mean of the previous 5-s values lower than P_{50} (μ) and dividing the result by μ. Positive calcium transients were identified following a two-step procedure: initially, $\Delta F/F$ traces were smoothened by convoluting the raw signal with a 10-s squared kernel. Using custom-written Matlab routines, true-positive NMDA transients (with a minimum of 1 s between transients) were defined on an automated basis where the threshold was set at 5*SD of APV average trace. Pairwise cross-correlation of transients between spines on the same neuron was computed using a time window of 0.5 s. We corrected the correlation values by subtracting the mean correlation obtained by shuffling the inter-transient time for individual spines (repeated 100 times).

Chemically induced potentiation (cLTP)

Live hippocampal neurons, cotransfected at 10 div with GluA1-SEP and Homer 1c–DsRed, were incubated (12 div) overnight with Env (1 μl/ml) or nothing (control) at 37°C. cLTP was provoked by bath co-application of 200 μM glycine (Tocris) and 5 μM picrotoxin (Tocris) for 4 min, as previously described (*24*). cLTP was always applied after a period (2 × 5 min) of baseline acquisition, and the medium was carefully replaced by fresh equilibrated and heated medium after induction. GluA1-SEP fluorescence signal was then recorded every 5 min during the following 30 min. Synapses were outlined using the synaptic Homer 1c signal, and GluA1-SEP intensity (ImageJ, NIH) was followed over time within these synaptic areas and then exclusively normalized to baseline if synapses showed a stable baseline (variation below 10% between −10 and −5 min). All images were collected on a video confocal spinning disk system (DMI6000B, Leica, Wetzlar, Germany) with a CoolSNAP HQ2 camera (Photometrics, Tucson, USA).

Animals

Pregnant rats (Sprague-Dawley) were purchased from Janvier (France), and P0 to P1 male pups from the same litter were assigned to different groups in a randomized manner: control, control+, or Env. Rats were kept at constant ambient temperature (21° ± 1°C) with ad libitum access to food and water. Every effort was made to minimize the number of animals used and their suffering. Animal procedures were conducted in accordance with the European Community guidelines (Directive 2010/63/EU) regulating animal research and were approved by the local Bordeaux Ethics Committee (APAFIS#3420-2015112610591204).

Postnatal electroporation was done in newborn pups between P0 and P1, as previously described. Briefly, pups were anesthetized by hypothermia and injected with DNA constructs coding for cytosolic EGFP to identify transfected cells (control group) in combination with an empty vector (control+ group) or with phCMV-MSRV Env (clone pV14, AF 331500) (Env group). Approximately 2 μg of DNA in 8 μl of PBS and 0.1 μl of Fast Green were injected into lateral ventricles, immediately followed by electroporation with five electrical pulses (150 V, 50-ms duration, and 1-s interval between pulses) delivered by a pulse generator (ECM 830; BTX, Harvard apparatus, San Diego, CA). Pups were reanimated on a thermal blanket at 37°C and quickly returned to their mother.

Behavioral responses

Experiments were conducted during the light cycle (14:00 to 20:00) by the same experimenter who handled the animals during their life span. Their weights were monitored every week, and at P21, the pups were weaned and housed two to five rats from the same litter and with the same treatment/cage.

Five different study groups were used: (i) The animals in the first group, control (n = 13) and Env (n = 13), were subjected to a series of behavioral tests in the following order: (a) at P35 to P37, locomotor activity and anxiety; (b) habituation/adaptation to the open field; (c) at P56 to P58, the PPI; and 2 days after, (d) social recognition and interaction. (ii) The animals in the second study group, control

(n = 30) and Env (n = 30), were exposed either to clozapine/vehicle treatment before PPI or to an MK-801 challenge on the day after PPI. (iii) The third study group, control (n = 11) and control+ (n = 14), was tested in the PPI, and (iv) the fourth study group, Env (n = 22), was subjected to a cross-link protocol (see below for stereotaxic injection) on the day before PPI. (v) The animals in the last group, control (n = 13) and Env (n = 24), were treated with the Env-neutralizing antibody during an early postnatal period. All animals were naïve to the apparatuses when first presented with the tests and acclimatized to the room for at least 1 hour before onset. Groups were pseudorandomized on each behavioral testing day. During the open field and PPI tests, the experimenter was not blind to the animal's condition although behavioral data collection was done using a fully computer-controlled setup and in an unbiased way. In contrast, the investigator was blinded to the treatment during scoring analysis in the social recognition and interaction test. See Fig. 4C for experimental layout.

Open field

Locomotor activity was measured in an open-field arena (54 cm long × 54 cm wide × 40 cm high) with light settings at approximately 5 lux. Novelty-induced locomotion was assessed by video tracking the rat that was allowed to freely explore the empty arena for 2 × 10 min on day 1 of three consecutive test days. From the recordings on day 1, anxiety was evaluated as the time spent within a center zone comprising 50% of the arena during the first 10 min. Then, habituation/adaptation to context was assessed as a decrease of locomotor activity on days 2 and 3. For MK-801 studies, control (n = 13) and Env (n = 12) rats were given an intraperitoneal injection with saline and left to explore the arena for 1 hour. Then, an MK-801 (0.5 mg/kg; Tocris) injection was administered intraperitoneally, and animals were monitored for two additional hours. One animal was excluded because of stereotypic behavior after injection. Total distance traveled was extracted with the idTracker software (*43*) and analyzed with automatized custom-written MATLAB routines.

Prepulse inhibition

PPI was performed using a Panlab startle chamber (Harvard, San Diego Instruments). Each PPI session lasted for approximately 31 min and began with a 5-min acclimatization period with a constant background noise. The session consisted of eight different trial types: a no pulse, a startle pulse (120 dB at 8 kHz, 40 ms) that was or was not preceded by three prepulses at +4, +8, and + 12 dB above a 74-dB background noise (20 ms, interval of 100 ms), and the prepulses alone. Each session started with 10 startle pulses [intertrial intervalls (ITIs) of 70 s] followed by a counterbalanced pseudorandom order of the 8 trials × 6 and ended by a final block of 10 startle pulses. Baseline data from different groups were initially pooled seeing that the effect of Env gene insertion on the overall PPI measured at the three prepulses was similar: (i) two-way analysis of variance (ANOVA), group factor; $F(1,72) = 11.23$, $^{**}P = 0.0013$, n = 13; and (ii) two-way ANOVA, group factor; $F(1,102) = 9.597$, $^{**}P = 0.0025$, n = 18. Potentiation in response to the prepulses was observed in both animal groups, and these animals were excluded from the final dataset. Prepulse inhibition is expressed as % PPI and was calculated by $(100*((S - PP)/S))$, where S = average response on startle-only trials and PP = average response on prepulse + startle trials. We confirmed that the DNA load was trivial to the behavioral outcome [study group (iii)] by comparing GFP animals with GFP + empty vector electroporated animals (fig. S6C).

In study group (ii), clozapine (Abcam, Cambridge, UK) (12 mg/kg) was dissolved in 0.1 N HCl and buffered with NaOH to pH 5.6, and a single intraperitoneal injection (1 ml/kg; clozapine or vehicle) was administered to control (n = 12) and Env (n = 12) animals 20 min before PPI evaluation (fig. S6D). Vehicle treatment did not affect PPI responses (data not shown). Stereotaxic injections were conducted in study group (iv) 1 day before the PPI test. Briefly, rats (P55 to P57) from the Env group were anesthetized with isoflurane and placed in a stereotaxic frame. Polyclonal goat anti-rabbit IgG (0.8 mg; 2 μl) (Novex, Thermo Fisher Scientific) (Env + Cont.IgG) (n = 13) or anti-rabbit GluN1 (Alomone Labs) (Env + GluN1 cross-link) (n = 11), diluted in 0.1% trypan blue (Sigma-Aldrich) (1:5), was stereotaxically injected into each hippocampus [coordinates relative to bregma, Anterior-Posterior (AP): −4.5 mm, Medial-Lateral (ML): ±3.2 mm, Dorsal-Ventral (DV): −2.0 mm]. On the basis of the cross-study coherence, the increased response to increased prepulse in all groups, and strong response at prepulse +8 dB, PPI data obtained from this prepulse are preferentially shown. The complete dataset can be seen in fig. S6E. Experiments from study groups (ii) to (iv) were executed in parallel. Early postnatal treatment was conducted by a single intraperitoneal injection of the Env-neutralizing antibody (30 mg/kg; GN_mAb_ENV_03; GeNeuro) or control antibody (30 mg/kg; GN_mAb_Gag_06; Geneuro) at P4, P8, and P12; animals were then left in their home cages until the day of PPI test at ~P58.

Social recognition and interaction

This protocol was adjusted from (*44*). The day before testing, three rats [one study rat (control or Env) and two target rats (naïve)] with similar weight (±5%) from different litters were assigned to be tested together. Target rats were then habituated to the experimental cage (a housing cage) in the experimental room for 1 hour. On the day of the experiment, the study rat was habituated to the experimental cage for 1 hour. Thereafter, without any training, the test started and the first target rat was placed into the same experimental cage (3 × 1 min, ITI 3 min), and social recognition was recorded. Subsequently, during the last interaction session, the first target rat was removed and the second target rat was placed into the experimental cage together with the study rat, and social interaction was recorded for 10 min. In the last session, control study rats showed increased interaction during the first minute, meaning that the rats were once again interested in the unfamiliar rat (second target rat). The full last session (10 min) was then scored to measure social interaction. Study and target rats were not used in this paradigm more than one time. Videos were scored in a blinded fashion for the time the study rat actively engaged in social-interacting behaviors (sniffing, grooming, close following, and crawling over/under). No aggressive behaviors were noted during the sessions.

Preparation of figures and analysis

Figures were assembled in ImageJ (NIH) and Adobe Photoshop (Adobe Systems, San Jose, CA); only contrast and brightness were adjusted to optimize the image quality. All statistical analysis was performed in GraphPad Prism 6 (GraphPad Software, San Diego, USA) and can be found in detail in table S2. In brief, statistical analysis using $\alpha = 0.5$ was conducted. For behavioral studies, a predetermined sample size was based on previous studies and the literature (*45*). Here, a sample size of 13 to 18 animals was used in the PPI, which corresponds to a power factor of 0.6 to 0.75 and α of 0.5, and in the cross-link and MK-801 experiments, a sample size of 11 animals corresponds to a power factor of 0.55 and <0.8, respectively. Parametric statistical tests were applied when data passed the D'Agostino and Pearson's omnibus normality test; hence, two-tailed Student's

t test with or without Welch's correction, one- or two-tailed paired Student's *t* test, or two-way ANOVA followed by Bonferroni's multiple comparisons test were conducted. Comparisons between groups with data from non-Gaussian distributions were performed using nonparametric test: either the two-tailed unpaired Mann-Whitney test or, for multiple groups, the Kruskal-Wallis test followed by Dunn's multiple comparison test. For direct comparison of distributions, Kolmogorov-Smirnov test was used. For behavioral testing, the PPI results were analyzed using the factors group and prepulse by two-way ANOVA followed by Bonferroni's multiple comparisons test for group and prepulse intensity. A one-way ANOVA followed by Tukey's multiple comparisons test for treatment was used in the cross-link and neutralizing antibody protocols. RM (repeated measures) two-way ANOVA considering the factors treatment and time followed by Fisher's least significant difference (LSD) post hoc analysis was used for the analysis of the MK-801 response, and a two-way ANOVA was used for TUNEL data with factors treatment and area. Significance levels were defined as $^{*}P < 0.05$, $^{**}P < 0.01$, and $^{***}P < 0.001$.

SUPPLEMENTARY MATERIALS

Supplementary material for this article is available at http://advances.sciencemag.org/cgi/content/full/6/29/eabc0708/DC1

View/request a protocol for this paper from *Bio-protocol*.

REFERENCES AND NOTES

1. E. B. Chuong, N. C. Elde, C. Feschotte, Regulatory evolution of innate immunity through co-option of endogenous retroviruses. *Science* **351**, 1083–1087 (2016).
2. C. Feschotte, E. J. Pritham, DNA transposons and the evolution of eukaryotic genomes. *Annu. Rev. Genet.* **41**, 331–368 (2007).
3. P. Küry, A. Nath, A. Creange, A. Dolei, P. Marche, J. Gold, G. Giovannoni, H. P. Hartung, H. Perron, Human endogenous retroviruses in neurological diseases. *Trends Mol. Med.* **24**, 379–394 (2018).
4. S. Chowdhury, J. D. Shepherd, H. Okuno, G. Lyford, R. S. Petralia, N. Plath, D. Kuhl, R. L. Huganir, P. F. Worley, Arc/Arg3.1 interacts with the endocytic machinery to regulate AMPA receptor trafficking. *Neuron* **52**, 445–459 (2006).
5. E. D. Pastuzyn, C. E. Day, R. B. Kearns, M. Kyrke-Smith, A. V. Taibi, J. McCormick, N. Yoder, D. M. Belnap, S. Erlendsson, D. R. Morado, J. A. G. Briggs, C. Feschotte, J. D. Shepherd, The neuronal gene Arc encodes a repurposed retrotransposon Gag protein that mediates intercellular RNA transfer. *Cell* **172**, 275–288 (2018).
6. N. Plath, O. Ohana, B. Dammermann, M. L. Errington, D. Schmitz, C. Gross, X. Mao, A. Engelsberg, C. Mahlke, H. Welzl, U. Kobalz, A. Stawrakakis, E. Fernandez, R. Waltereit, A. Bick-Sander, E. Therstappen, S. F. Cooke, V. Blanquet, W. Wurst, B. Salmen, M. R. Bosl, H. P. Lipp, S. G. Grant, T. V. Bliss, D. P. Wolfer, D. Kuhl, Arc/Arg3.1 is essential for the consolidation of synaptic plasticity and memories. *Neuron* **52**, 437–444 (2006).
7. R. Ono, K. Nakamura, K. Inoue, M. Naruse, T. Usami, N. Wakisaka-Saito, T. Hino, R. Suzuki-Migishima, N. Ogonuki, H. Miki, T. Kohda, A. Ogura, M. Yokoyama, T. Kaneko-Ishino, F. Ishino, Deletion of Peg10, an imprinted gene acquired from a retrotransposon, causes early embryonic lethality. *Nat. Genet.* **38**, 101–106 (2006).
8. Y. Sekita, H. Wagatsuma, K. Nakamura, R. Ono, M. Kagami, N. Wakisaka, T. Hino, R. Suzuki-Migishima, T. Kohda, A. Ogura, T. Ogata, M. Yokoyama, T. Kaneko-Ishino, F. Ishino, Role of retrotransposon-derived imprinted gene, Rtl1, in the feto-maternal interface of mouse placenta. *Nat. Genet.* **40**, 243–248 (2008).
9. R. N. Douville, A. Nath, Human endogenous retroviruses and the nervous system. *Handb. Clin. Neurol.* **123**, 465–485 (2014).
10. W. Li, M. H. Lee, L. Henderson, R. Tyagi, M. Bachani, J. Steiner, E. Campanac, D. A. Hoffman, G. von Geldern, K. Johnson, D. Maric, H. D. Morris, M. Lentz, K. Pak, A. Mammen, L. Ostrow, J. Rothstein, A. Nath, Human endogenous retrovirus-K contributes to motor neuron disease. *Sci. Transl. Med.* **7**, 307ra153 (2015).
11. H. Karlsson, S. Bachmann, J. Schroder, J. McArthur, E. F. Torrey, R. H. Yolken, Retroviral RNA identified in the cerebrospinal fluids and brains of individuals with schizophrenia. *Proc. Natl. Acad. Sci. U.S.A.* **98**, 4634–4639 (2001).
12. F. Li, S. Sabunciyan, R. H. Yolken, D. Lee, S. Kim, H. Karlsson, Transcription of human endogenous retroviruses in human brain by RNA-seq analysis. *PLOS ONE* **14**, e0207353 (2019).
13. H. Perron, L. Mekaoui, C. Bernard, F. Veas, I. Stefas, M. Leboyer, Endogenous retrovirus type W GAG and envelope protein antigenemia in serum of schizophrenic patients. *Biol. Psychiatry* **64**, 1019–1023 (2008).
14. M. Leboyer, R. Tamouza, D. Charron, R. Faucard, H. Perron, Human endogenous retrovirus type W (HERV-W) in schizophrenia: A new avenue of research at the gene-environment interface. *World J. Biol. Psychiatry* **14**, 80–90 (2013).
15. G. Slokar, G. Hasler, Human endogenous retroviruses as pathogenic factors in the development of schizophrenia. *Front. Psychol.* **6**, 183 (2015).
16. A. Sekar, A. R. Bialas, H. de Rivera, A. Davis, T. R. Hammond, N. Kamitaki, K. Tooley, J. Presumey, M. Baum, D. Van, G. Genovese, S. A. Rose, R. E. Handsaker, M. J. Daly, M. C. Carroll, B. Stevens, S. A. McCarroll, Schizophrenia risk from complex variation of complement component 4. *Nature* **530**, 177–183 (2016).
17. C. M. Sellgren, J. Gracias, B. Watmuff, J. D. Biag, J. M. Thanos, P. B. Whittredge, T. Fu, K. Worringer, H. E. Brown, J. Wang, A. Kaykas, R. Karmacharya, C. P. Goold, S. D. Sheridan, R. H. Perlis, Increased synapse elimination by microglia in schizophrenia patient-derived models of synaptic pruning. *Nat. Neurosci.* **22**, 374–385 (2019).
18. K. Nakazawa, V. Jeevakumar, K. Nakao, Spatial and temporal boundaries of NMDA receptor hypofunction leading to schizophrenia. *NPJ Schizophr.* **3**, 7 (2017).
19. P. Paoletti, C. Bellone, Q. Zhou, NMDA receptor subunit diversity: Impact on receptor properties, synaptic plasticity and disease. *Nat. Rev. Neurosci.* **14**, 383–400 (2013).
20. J. H. Krystal, A. Anticevic, G. J. Yang, G. Dragoi, N. R. Driesen, X. J. Wang, J. D. Murray, Impaired tuning of neural ensembles and the pathophysiology of schizophrenia: A translational and computational neuroscience perspective. *Biol. Psychiatry* **81**, 874–885 (2017).
21. E. M. Poels, L. S. Kegeles, J. T. Kantrowitz, M. Slifstein, D. C. Javitt, J. A. Lieberman, A. Abi-Dargham, R. R. Girgis, Imaging glutamate in schizophrenia: Review of findings and implications for drug discovery. *Mol. Psychiatry* **19**, 20–29 (2014).
22. F. Komurian-Pradel, G. Paranhos-Baccala, F. Bedin, A. Ounanian-Paraz, M. Sodoyer, C. Ott, A. Rajoharison, E. Garcia, F. Mall, B. Mandrand, H. Perron, Molecular cloning and characterization of MSRV-related sequences associated with retrovirus-like particles. *Virology* **260**, 1–9 (1999).
23. H. Perron, B. Lalande, B. Gratacap, A. Laurent, O. Genoulaz, C. Geny, M. Mallaret, E. Schuller, P. Stoebner, J. M. Seigneurin, Isolation of retrovirus from patients with multiple sclerosis. *Lancet* **337**, 862–863 (1991).
24. J. P. Dupuis, L. Ladepeche, H. Seth, L. Bard, J. Varela, L. Mikasova, D. Bouchet, V. Rogemond, J. Honnorat, E. Hanse, L. Groc, Surface dynamics of GluN2B-NMDA receptors controls plasticity of maturing glutamate synapses. *EMBO J.* **33**, 842–861 (2014).
25. L. Groc, M. Heine, S. L. Cousins, F. A. Stephenson, B. Lounis, L. Cognet, D. Choquet, NMDA receptor surface mobility depends on NR2A-2B subunits. *Proc. Natl. Acad. Sci. U.S.A.* **103**, 18769–18774 (2006).
26. A. Rolland, E. Jouvin-Marche, C. Viret, M. Faure, H. Perron, P. N. Marche, The envelope protein of a human endogenous retrovirus-W family activates innate immunity through CD14/TLR4 and promotes Th1-like responses. *J. Immunol.* **176**, 7636–7644 (2006).
27. M. W. Salter, L. V. Kalia, Src kinases: A hub for NMDA receptor regulation. *Nat. Rev. Neurosci.* **5**, 317–328 (2004).
28. A. J. Watt, M. C. van Rossum, K. M. MacLeod, S. B. Nelson, G. G. Turrigiano, Activity coregulates quantal AMPA and NMDA currents at neocortical synapses. *Neuron* **26**, 659–670 (2000).
29. H. Grea, D. Bouchet, V. Rogemond, N. Hamdani, E. Le Guen, R. Tamouza, E. Darrau, C. Passerieux, J. Honnorat, M. Leboyer, L. Groc, Human autoantibodies against N-methyl-D-aspartate receptor modestly alter dopamine D1 receptor surface dynamics. *Front. Psychol.* **10**, 670 (2019).
30. L. Ladepeche, J. P. Dupuis, D. Bouchet, E. Doudnikoff, L. Yang, Y. Campagne, E. Bézard, E. Hosy, L. Groc, Single-molecule imaging of the functional crosstalk between surface NMDA and dopamine D1 receptors. *Proc. Natl. Acad. Sci. U.S.A.* **110**, 18005–18010 (2013).
31. C. A. Jones, D. J. Watson, K. C. Fone, Animal models of schizophrenia. *Br. J. Pharmacol.* **164**, 1162–1194 (2011).
32. R. Birnbaum, D. R. Weinberger, Genetic insights into the neurodevelopmental origins of schizophrenia. *Nat. Rev. Neurosci.* **18**, 727–740 (2017).
33. O. Marin, Developmental timing and critical windows for the treatment of psychiatric disorders. *Nat. Med.* **22**, 1229–1238 (2016).
34. F. Gardoni, M. Boraso, E. Zianni, E. Corsini, C. L. Galli, F. Cattabeni, M. Marinovich, M. Di Luca, B. Viviani, Distribution of interleukin-1 receptor complex at the synaptic membrane driven by interleukin-1beta and NMDA stimulation. *J. Neuroinflammation* **8**, 14 (2011).
35. M. Potier, F. Georges, L. Brayda-Bruno, L. Ladepeche, V. Lamothe, A. S. Al Abed, L. Groc, A. Marighetto, Temporal memory and its enhancement by estradiol requires surface dynamics of hippocampal CA1 N-methyl-D-aspartate receptors. *Biol. Psychiatry* **79**, 735–745 (2016).

36. D. Kremer, J. Gruchot, V. Weyers, L. Oldemeier, P. Göttle, L. Healy, J. Ho Jang, Y. K. T. Xu, C. Volsko, R. Dutta, B. D. Trapp, H. Perron, H.-P. Hartung, P. Küry, pHERV-W envelope protein fuels microglial cell dependent damage of myelinated axons in multiple sclerosis. *Proc. Natl. Acad. Sci. U.S.A.* **30**, 15216–15225 (2019).
37. R. R. Girgis, S. S. Kumar, A. S. Brown, The cytokine model of schizophrenia: Emerging therapeutic strategies. *Biol. Psychiatry* **75**, 292–299 (2014).
38. B. Viviani, S. Bartesaghi, F. Gardoni, A. Vezzani, M. M. Behrens, T. Bartfai, M. Binaglia, E. Corsini, M. Di Luca, C. L. Galli, M. Marinovich, Interleukin-1beta enhances NMDA receptor-mediated intracellular calcium increase through activation of the Src family of kinases. *J. Neurosci.* **23**, 8692–8700 (2003).
39. D. Saylor, A. M. Dickens, N. Sacktor, N. Haughey, B. Slusher, M. Pletnikov, J. L. Mankowski, A. Brown, D. J. Volsky, J. C. McArthur, HIV-associated neurocognitive disorder—Pathogenesis and prospects for treatment. *Nat. Rev. Neurol.* **12**, 234–248 (2016).
40. B. Viviani, F. Gardoni, S. Bartesaghi, E. Corsini, A. Facchi, C. L. Galli, M. Di Luca, M. Marinovich, Interleukin-1 beta released by gp120 drives neural death through tyrosine phosphorylation and trafficking of NMDA receptors. *J. Biol. Chem.* **281**, 30212–30222 (2006).
41. J. Ashley, B. Cordy, D. Lucia, L. G. Fradkin, V. Budnik, T. Thomson, Retrovirus-like Gag protein Arc1 binds RNA and traffics across synaptic boutons. *Cell* **172**, 262–274.e11 (2018).
42. G. M. Khandaker, L. Cousins, J. Deakin, B. R. Lennox, R. Yolken, P. B. Jones, Inflammation and immunity in schizophrenia: Implications for pathophysiology and treatment. *Lancet Psychiatry* **2**, 258–270 (2015).
43. A. Perez-Escudero, J. Vicente-Page, R. C. Hinz, S. Arganda, G. G. de Polavieja, idTracker: Tracking individuals in a group by automatic identification of unmarked animals. *Nat. Methods* **11**, 743–748 (2014).
44. H. Huang, C. Michetti, M. Busnelli, F. Manago, S. Sannino, D. Scheggia, L. Giancardo, D. Sona, V. Murino, B. Chini, M. L. Scattoni, F. Papaleo, Chronic and acute intranasal oxytocin produce divergent social effects in mice. *Neuropsychopharmacology* **39**, 1102–1114 (2014).
45. N. R. Swerdlow, G. A. Light, M. R. Breier, J. M. Shoemaker, R. L. Saint Marie, A. C. Neary, M. A. Geyer, K. E. Stevens, S. B. Powell, Sensory and sensorimotor gating deficits after neonatal ventral hippocampal lesions in rats. *Dev. Neurosci.* **34**, 240–249 (2012).

Acknowledgments: We thank J. Jezequel for critical input, D. Jercog for help with imaging analysis, and laboratory members for constructive discussions. We also thank the Bordeaux Imaging Centre (service unit of the CNRS-INSERM and Bordeaux University, member of the national infrastructure France BioImaging), Pole in vivo for animal care, and the Biochemistry and Biophysics Platform of the Bordeaux Neurocampus. **Funding:** This work was supported by the National Center for Scientific Research (CNRS), Agence Nationale de la Recherche, Fondation FondaMental, Fondation pour la Recherche Médicale (DPP20151033969), Conseil Régional d'Aquitaine, Stiftelsen Olle Engkvist Byggmästare, and Svensk-Franska Stiftelsen.
Author contributions: Conceptualization: E.M.J., M.L., H.P., and L.G. Methodology: E.M.J. and L.G. Formal analysis/investigation: E.M.J., D.B., P.E., AS.M., E.A., and R.G. Resources: R.T., R.G., M.L., H.P., and L.G. Writing (original draft): E.M.J. and L.G. Writing (review and editing): E.M.J., R.T., P.E., E.A., R.G., M.L., H.P., and L.G. Supervision: L.G. Project administration: L.G. Funding acquisition: E.M.J., M.L., H.P., and L.G. **Competing interests:** H.P. receives compensation for his work as CSO from GeNeuro. The authors declare that they have no other competing interests. **Data and materials availability:** All data needed to evaluate the conclusions in the paper are present in the paper and/or the Supplementary Materials. Additional data related to this paper may be requested from the authors.

Submitted 4 April 2020
Accepted 4 June 2020
Published 17 July 2020
10.1126/sciadv.abc0708

Citation: E. M. Johansson, D. Bouchet, R. Tamouza, P. Ellul, AS. Morr, E. Avignone, R. Germi, M. Leboyer, H. Perron, L. Groc, Human endogenous retroviral protein triggers deficit in glutamate synapse maturation and behaviors associated with psychosis. *Sci. Adv.* **6**, eabc0708 (2020).